PINSTECH/NED-134

In-Core Neutron Flux Measurements at PARR Using Self Powered Neutron Detectors

Amjad Hassain
Saleem A. Ansari

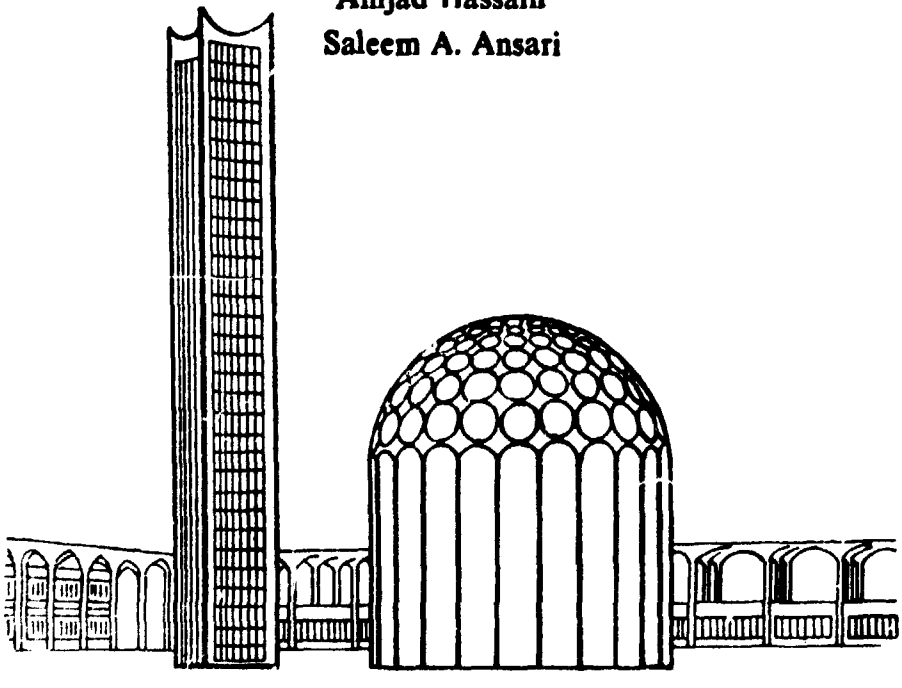

NUCLEAR ENGINEERING DIVISION
Pakistan Institute of Nuclear Science & Technology
P. O. Nilore Islamabad.
October 1989

PINSTECH/NED-134

In-Core Neutron Flux Measurements at PARR using Self Powered Neutron Detectors

Amjad Hussain
Saleem A. Ansari

Nuclear Engineering Division
Pakistan Institute of Nuclear Science and Technology
P.O. Nilore
Islamabad
October, 1989

Abstract

This report describes experimental reactor physics measurements at PARR using the in-core neutron detectors. Rhodium self powered neutron detectors (SPND) were used in the PARR core and several measurements were made aimed at detector calibration, response time determination and neutron flux measurements. The detectors were calibrated at low power using gold foils and full power by the thermal channel. Based on this calibration it was observed that the detector response remains almost linear throughout the power range. The self powered detectors were used for on-line determination of absolute neutron flux in the core as well as the spatial distribution of the neutron flux or reactor power. The experimental, axial and horizontal flux mapping results at certain locations in the core are presented. The total response time of the Rhodium detectors was experimentally determined to be about 5 minutes, which agrees well with the theoretical results. Because of longer response time of the SPND detectors it is not possible to use them in the reactor protection system.

LIST OF CONTENTS

1.0 Introduction

Self powered neutron detectors are in widespread use in nuclear reactors as in-core detectors[1,2,3]. The main function of these detectors is to provide power distribution information under different operating conditions, e.g. control rod changes, fuel burn-up and reactor poisons. This information is necessary for fuel burn-up optimization and reactor safety. Self powered neutron detectors are primarily activation detectors and their construction avoids the problems of high voltage or gas leakage. Because of their low sensitivity the detector burn-up is relatively low, which increases the life of the detector in the reactor. Also because of their small diameter (of the order of a few millimeters) these detectors can be used conveniently in those core locations which are otherwise difficult to access. However, the low sensitivity of these detectors imposes a limit on the measurement of low flux.

1.1 Theory of Detection

The most common detector form for SPND is a coaxial cylinder with an emitter in the center surrounded completely by an insulator and the outer sheath which acts as collector, as shown in Fig. 1. Table I gives a summary of the commonly used emitter materials for self powered neutron detectors [4].

The emitter material must have an appropriate neutron absorption cross section, which usually is a compromise between detector sensitivity and detector burn-up. Other emitter material selection criteria are the energy of the radiation emitted after neutron capture, the half life of the produced radio-nuclides and their daughter products.

The insulator usually consists of a high temperature resistant material like Al_2O_3, MgO or BeO, and must have a thickness that allows the produced electrons to reach the collector [4].

The collector has to collect the emitted electrons and gives the detector its mechanical stability. It must be corrosion resistant

Table I - Emitter materials for Self-Powered Neutron Detectors

Material	Abundance (%)	Activation cross-section (barns)	Half life	Maximum beta energy (MeV)	Burn-up at 10^{13} neutrons ($cm^{-2}.sec^{-1}$)
^{7}Li	92.58	0.036	0.855 sec	13.0	Negligible
^{11}B	80.4	0.005	0.025 sec	13.4	Negligible
^{27}Al	100	0.230	2.30 min	2.87	Negligible
^{51}V	99.76	4.9	3.76 min	2.47	0.013%/month
^{55}Mn	100	13.3	2.58 hr	2.85	0.035%/month
^{99}Tc	Artificial	22	16 sec	3.37	0.058%/month
^{103}Rh	100	139	42 sec	2.44	0.40%/month
		11	4.4 min		
^{115}In	95.72	154	54 min	1.0	0.53%/month
		45	14 sec		
^{109}Ag	48.18	92	24 sec	2.87	0.24%/month
^{107}Ag	51.82	35	2.4 min	1.64	0.092%/month

and should not undergo dimensional changes at high temperatures. After a neutron capture in the emitter a (n,Y)(Y,e) reaction produces electrons. The constant loss of electrons from the emitter produces a small current between emitter and collector which can be measured directly with the help of an electrometer. The current output is directly proportional to the rate of absorption of neutrons in the emitter and thus proportional to the neutron flux at the surface of the detector.

When the activity induced in the emitter due to activation by thermal neutron flux is from one nuclide resulting in one half life, the spontaneous detector current, $I_{(t)}$, after exposure to thermal neutron flux, ϕ, for a time t is given by,

$$I_{(t)} = K \sigma_a Q N [1 - \exp(-\lambda t)] \quad (1)$$

where,

K = dimensionless constant determined by detector geometry and materials

σ_a = thermal-neutron activation cross section of emitter material (cm^2)

Q = Charge emitted by emitter per neutron absorbed(Coulomb)

N = number of emitter atoms

λ = decay constant of radionuclide generated in emitter (sec^{-1})

The output current of self powered neutron detector lags behind the input neutron flux and there exists a delay between the detector input and output. The time response curve for a typical SPND to a step input is shown in Fig. 2 [5].
The time constant τ, of the detector is defined as the time in which the output reaches the 63.2% of the final response after the step input. The detector response $R_{(t)}$ at any time t after the step input is given by

$$R_{(t)} = R_i + (R_f - R_i)[1 - \exp(-t/\tau)]$$

where R_i and R_f are the detector output current before step input and the final response respectively.

2.0 Experimental Arrangements

2.1 SPND for PARR

For reactor physics measurements at PARR an assembly containing three identical self-powered neutron detectors was used. The detector emitters are made of rhodium-103 (the related data about rhodium is given in table I). Each detector is 81 mm long and has a diameter of 1.4 mm. The outer sheath or the collector is made of Inox with the insulation resistance of the order of tera ohms. The schematics of the whole detector assembly is shown in Fig. 3. All three detectors are encapsulated in an Inox tube

whose outer diameter is 5 mm. The spacing between the centers of two adjacent detectors is 200 mm. Three co-axial cables terminated by BNC connectors come out of the Inox tube for the measurement of detector output currents. For water tightness the cables are enclosed in a vinyl pipe.

In order to avoid any damage to the detectors during handling, a detector handling assembly was fabricated locally. It consisted of a 8 meters long aluminium pipe having an outer diameter of 2.5 cm. The SPND assembly was mounted on this pipe with the help of two aluminum clamps, and the plastic tube containing the detector cables was fixed to the pipe surface. The length of the aluminum pipe was sufficient for easy handling even when the detector assembly was seated on the grid plate.

2.2 Detector Calibration

The output sensitivity (amperes per unit neutron flux) data of the self powered neutron detectors used in PARR was not available. It was essential to calibrate the detectors very carefully, since the accuracy of all flux measurements depend on this calibration. Each detector was calibrated separately in the reactor using gold foil activation technique, as described later. The gamma detection system used for foil counting consisted of a Canberra Ge(Li) detector with prefixed pre-amplifier, associated electronics, high voltage supply and a Canberra model 8180 multichannel analyzer (MCA) unit. The Ge(Li) detector had an operating voltage of 4 kV. The absolute efficiency and energy calibration of the detector was determined with the help of a wide energy range gamma source. The detector efficiency was calculated to be 0.00193 at 20 cm distance, whereas the energy resolution (full width half maximum) of the gamma peak was determined as 1.7 keV at 661 keV gamma energy.

3.0 Results and Discussion

3.1 Linearity Of SPND Current with Reactor Power

In order to investigate the behavior of detector current with the neutron flux, output current of each detector was measured at

different power levels. For this purpose the SPND assembly was lowered into the reactor core at location D3 and The reactor power was raised up to full power of 5 MW from shut-down in several steps. The detector location and core configuration is shown in Fig. 4. For each measurement the reactor power was allowed to stabilize at a constant level and the detector output currents were measured over a period of few minutes to obtain the saturated value at the particular power. It was observed that the detector current started increasing from the background value at about 1 kW power level. The measured data for the three detectors at power levels is presented in table II.

Table II - Output Current of SPND's at Different Power Levels when Detector Assembly is Placed at Position D3

Reactor power	Output current (A)		
	SPND no. 1	SPND no. 2	SPND no. 3
1 kW	$.27\times10^{-10}$	$.6\times10^{-10}$	$.4\times10^{-9}$
5 kW	1.5×10^{-10}	2.6×10^{-10}	$.62\times10^{-9}$
50 kW	1.5×10^{-9}	3.2×10^{-9}	3.2×10^{-9}
500 kW	1.46×10^{-8}	2.5×10^{-8}	3×10^{-8}
5 MW	1.5×10^{-7}	2.9×10^{-7}	2.9×10^{-7}

Note that detector currents vary linearly with the reactor power over almost the entire power range.

To determine the detector behavior under abnormal flux conditions, the above experimental measurements were repeated with control rod no. 5 in both fully seated and fully out position. Control rod no. 5 was chosen because of its maximum reactivity worth and proximity to the SPND location. The curves of detector no. 2 output current vs reactor power for all three conditions are plotted in Fig. 5. Note that for different flux shapes the detector current still varies linearly with the

reactor power but the slopes of the three curves are markedly different from each other.

3.2 Response Time Measurements

In order to measure the response time of SPND, both positive and negative reactivity ramp inputs were introduced in the reactor core and detectors' response were recorded on a linear chart recorder. The reactor power was initially levelled at 5 kW and a positive reactivity ramp of 0.16 % Δ k/k was applied for about 24 seconds duration. The reactor power increased with a corresponding period of 30 seconds and it was levelled again at 70 kW. The detector response was recorded till it reached the stable value corresponding to the final power. The input reactivity change was also recorded with the help of plant reactivity meter. Fig. 6 gives the reactivity plot and the corresponding detector response curve vs. time (curves I & II). The logarithmic scale is used for detector output so that the exponential response function can be represented by straight lines on the plot. Following points are evident from Fig. 6.

1. The SPND takes about 10 seconds to respond initially to the input reactivity change.
2. The later response of SPND can be represented by two straight lines of different slopes. The detector output reaches 66% of its final value in a relative short time of 2 minutes. This agrees well with the time of 80 seconds required for the reactor power to reach the stable 70 kW value with the period of 30 seconds. The remaining 33% of the detector response accomplishes in about 3 minutes time. The detector output therefore requires a total of 5 minutes to reach the final stable value. A similar behavior was also observed for the other two detectors.

The detector response to the negative reactivity change is essentially the same as that for positive values and is shown in Fig. 6 (curve III). The total time of fall of reactor power from 74 kW to 12 kW in case of negative reactivity insertion is about 6 minutes, which includes the relatively slow power change caused by the delayed neutrons.

3.3 Determination of Detector Sensitivity

As discussed in section 2.2 the sensitivity of each detector was experimentally determined in the reactor using foil activation technique. Square gold foils having 1 sq cm area, 125 micron thickness and weighing 0.25 g were used for this purpose. The gold foils were mounted at the center of each detector and the detector assembly was lowered in reactor core at position D3 in such a way that the gold foils faced towards the core. The reactor was operated at a power of 50 kW stable power and the foils were irradiated for about 5 minutes. Current from each SPND was also measured at steady state reactor power. The SPND assembly was removed from reactor core and after proper cooling time the irradiated gold foils were counted in the counting set-up described earlier.

The absolute neutron flux, ϕ, was calculated from the measured foil activity using the following relation [6]

$$\phi = \frac{C_{(t)} * e^{198\lambda\, t_d}}{\varepsilon * t_{irr} * {}^{198}_{\lambda} * {}^{197}N * {}^{197}\sigma_a} \qquad (3)$$

where,

σ_a = activation cross section of Au-197 (96 barns)

t_{irr} = irradiation time of gold foils in seconds

^{197}N = total number of Au-197 atoms before irradiation

^{198}A = activity of Au-198 #/sec at the time of irradiation

$^{198}\lambda$ = decay constant of Au-198 (sec^{-1})

$C_{(t)}$ = counts per sec full peak from Ge(Li) detector

ε = efficiency of Ge(Li) detector at the foil distance

t_d = decay time or cooling time, in seconds

Since the gold foils available for irradiation had the thickness of 125 microns, the self shielding phenomenon may induce an error in the flux calculation. The self shielding factor for the particular foil thickness was calculated using the formulae given in literature [6]. The value of this correction factor for the

particular foil thickness was determined to be 0.87. To cross-check the flux calculations obtained by foil activation the same gold foils were counted in another gamma detection set-up in NCD and the two measurement results were in good agreement with each other. The measured, absolute neutron fluxes (after correction) incident at each detector in location D3 are tabulated in table III along with the sensitivity of the SPND detectors. The detector sensitivity is obtained by dividing the observed detector current by the measured neutron flux. It might be mentioned that the detector sensitivity obtained per unit sensitive length agrees well with the values cited in the literature [4] for the same dimensions.

Table III - Absolute Thermal Neutron Flux Incident on the Gold Foils. Reactor Power was 50 kW.

SPND no.	Corrected neutron flux (#/cm^2/sec)	Detector current (A)	Detector Sensitivity* A/(#/cm2/sec)/cm
1	2.33×10^{11}	2.4×10^{-9}	2.1×10^{-21}
2	3.15×10^{11}	3.6×10^{-9}	2.3×10^{-21}
3	1.97×10^{11}	2.8×10^{-9}	2.8×10^{-21}

* Effective detector length = 5 cm.

3.4 Neutron Flux Distribution

Since the main purpose of self powered neutron detectors is on-line flux mapping in reactor core, these measurements will be discussed in detail. The neutron fluxes were measured at the selected points in and around PARR core in both vertical (axial) and horizontal direction. The results of these measurements are given below.

3.4.1 Axial Flux Mapping

For determination of vertical flux distribution the SPND assembly was lowered in position D3 in the reactor core such that the

lower end of the detector assembly was seated at the grid plate. D3 location was particularly selected since most of the samples are irradiated in this position (see Fig. 4) and it is necessary to obtain precise information about the axial flux distribution at this location. In order to scan the entire core height, the assembly was raised from its lowest position in the core in 5 cm steps and the output currents from the three detectors were recorded under stable power conditions at full power. The neutron flux in each case was calculated using the individual detector sensitivity. The axial flux distribution obtained by all three detectors are plotted in Fig. 7 as a function of core height. The relevant data for detector no.3 is given in table IV. Following facts are evident from Fig. 7.

1. The axial neutron flux has a cosine distribution having a maxima between 36 to 42 cm from the bottom of the core (grid plate). The peak absolute neutron flux obtained by detector no. 3 comes out to be 2.7×10^{13} #/cm^2/sec.

2. The neutron fluxes obtained by the upper two detectors (SPND no. 1 & 2) are in good agreement with each other over the entire core height (78 cm). The two detectors' outputs start deviating from each other in the water reflector region at the top of the core. The flux distribution obtained by the lowermost (no. 3) detector shows higher values than the other two detectors especially in the reflector region. The reason for this deviation can be attributed to the fact that as the lowermost detector is raised above the core the whole assembly comes out of the reactor core and the fixed horizontal position of the detectors cannot be ensured.

The distribution of neutron flux under abnormal operating conditions were also measured at location D-3 by withdrawing the shim rod no. 5 fully out at full power level and then seating shim rod no. 5. Rod no. 5 was selected because of the same reasons as given in section 3.1. The axial flux distribution in the two extreme cases is plotted in Fig. 8 and Fig. 9.

Table IV - Axial Flux Mapping data at Position D3
(Output of SPND no. 3 at full power)

Distance from the bottom of core (cm)	Output current($x10^7$) (A)	Neutron Flux $x10^{-13}$ ($\#/cm^2/sec$)
11	2.5	1.8
21	3.2	2.3
31	3.6	2.6
41	3.8	2.7
51	3.4	2.4
61	2.8	2.0
71	1.8	1.3
81	1.4	1.0

3.4.2 Flux Mapping in Horizontal Direction

The horizontal distribution of neutron flux was measured at the core peripheral position along the open side of the core. For this purpose the SPND assembly was lowered at different points on the grid plat at locations A-1 to F-1, and the three detector currents at each location were recorded. The corresponding neutron fluxes for the middle (no. 2) detector are plotted as a function of horizontal distance in Fig. 10. (The origin of the x-axis coincides with the grid location A-1). The horizontal flux distribution in the reflector region also exhibits a cosine shape with a rather broad maxima. As expected, the flux falls off sharply at the corners of the core.

4. Conclusion

The utilization of the self powered neutron detector for in-core neutron flux measurements has been demonstrated at PARR. It has been shown that once the sensitivity of the detectors is determined accurately, these can be utilized conveniently for the determination of flux profile and local power distribution in the core. The on-line determination of these factors avoids major problems associated with the gold foils. It is planned to use these detector for the new up-graded PARR core in future.

5. References

1. Bock, H.
"Miniature Detectors for Reactor in-Core Neutron Flux Monitoring"
Atomic Energy Review, 141(1976)

2. Allen C.J et. al.
"Recent Advances in Self Powered Flux Detector Development for CANDU Reactors"
IAEA-SM-265/8

3. "In-Core Instrumentation and Reactor Assessment"
OCDE Proceedings of Specialists Meeting, Paris, 1984

4. Nuclear Power Reactor Instrumentation Systems Handbook Vol.2
U.S. Atomic Energy Commission, 1974

5. Curtis D. Johnson,
"Process Control Instrumentation Technology"
John Wiley & Sons, New York, USA, (1982)

6. Edward Profio, A.
"Experimental Reactor Physics"
John Wiley & Sons, New York, USA 1976

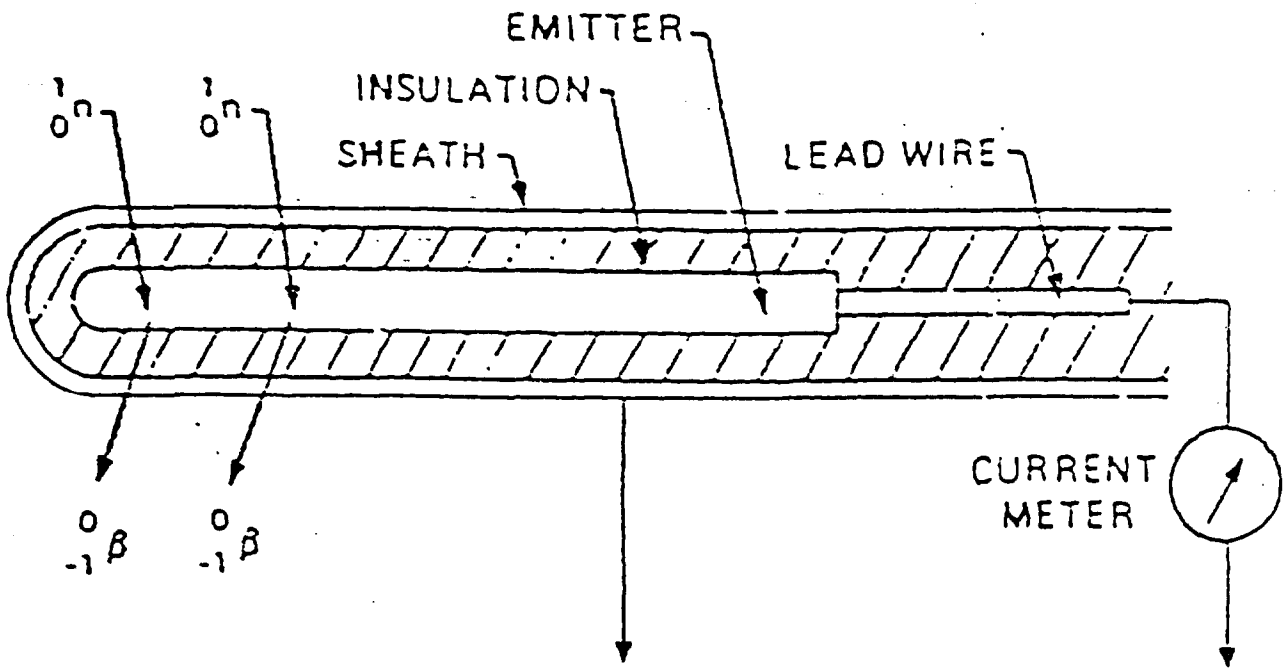

Fig. 1 : Construction and Operating Principle of SPND

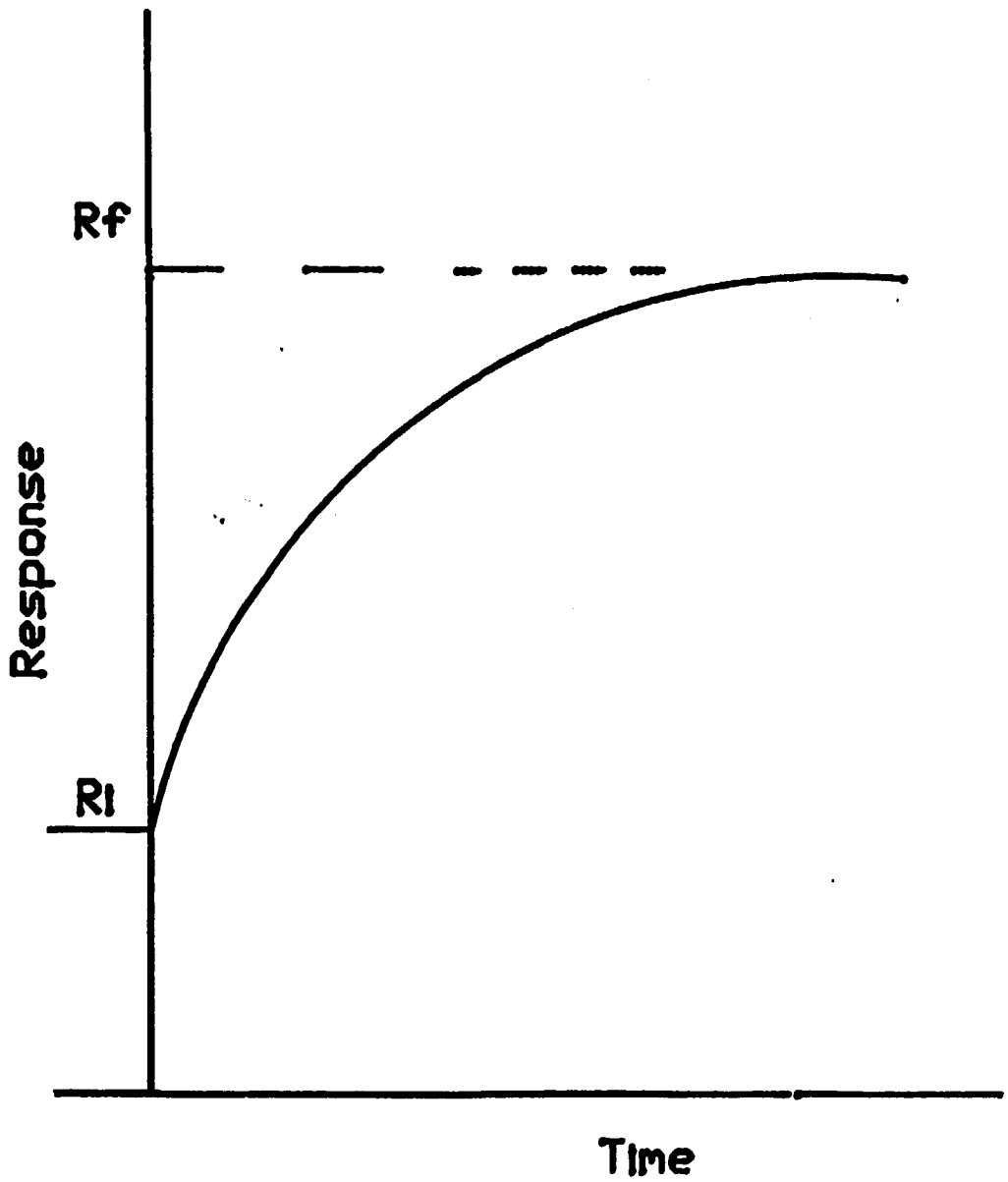

Fig. 2: Typical Response of SPND Detector for Step Power Input

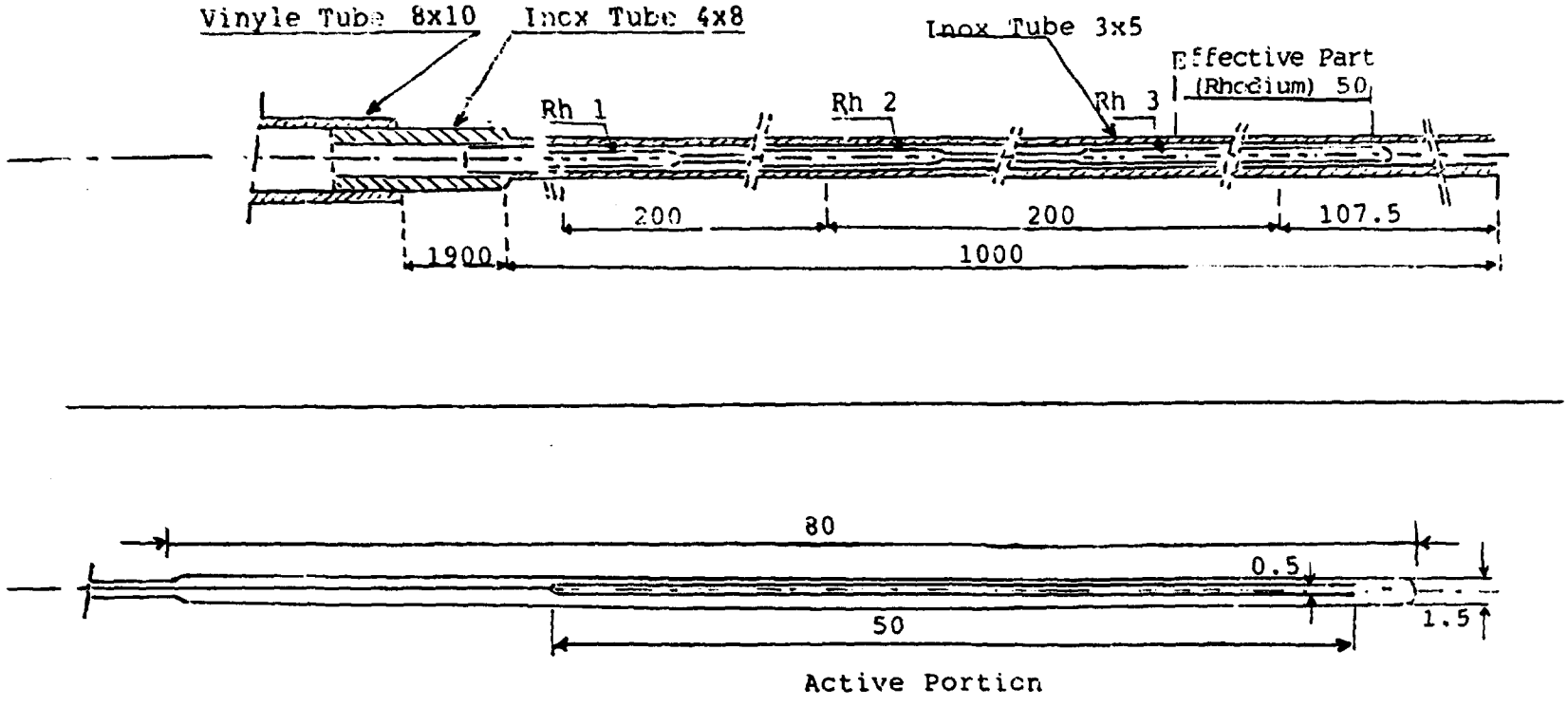

All demensions in mm

Fig. 3: Schematic Diagram of SPND for PARR

	1	2	3	4	5	6	7	8	9
A		GR-08	GR-10	S-54	S-65	S-58	S-49	S-50	S-51
B		GR-02	FC	S-53	S-56	C-13	S-52	C-14	S-09
C		GR-17	GR-14	S-63	S-61	S-60	C-16	S-57	S-17
D		GR-16		S-64	S-62	C-17	S-22	C-10	S-47
E		GR-06	GR-11	S-39	S-59	S-55	C-15	S-27	S-48
F		GR-07	FC	S-37	S-24	S-31	S-43	S-44	S-45

Fig. 4 : PARR Core Configuration Showing Location D3

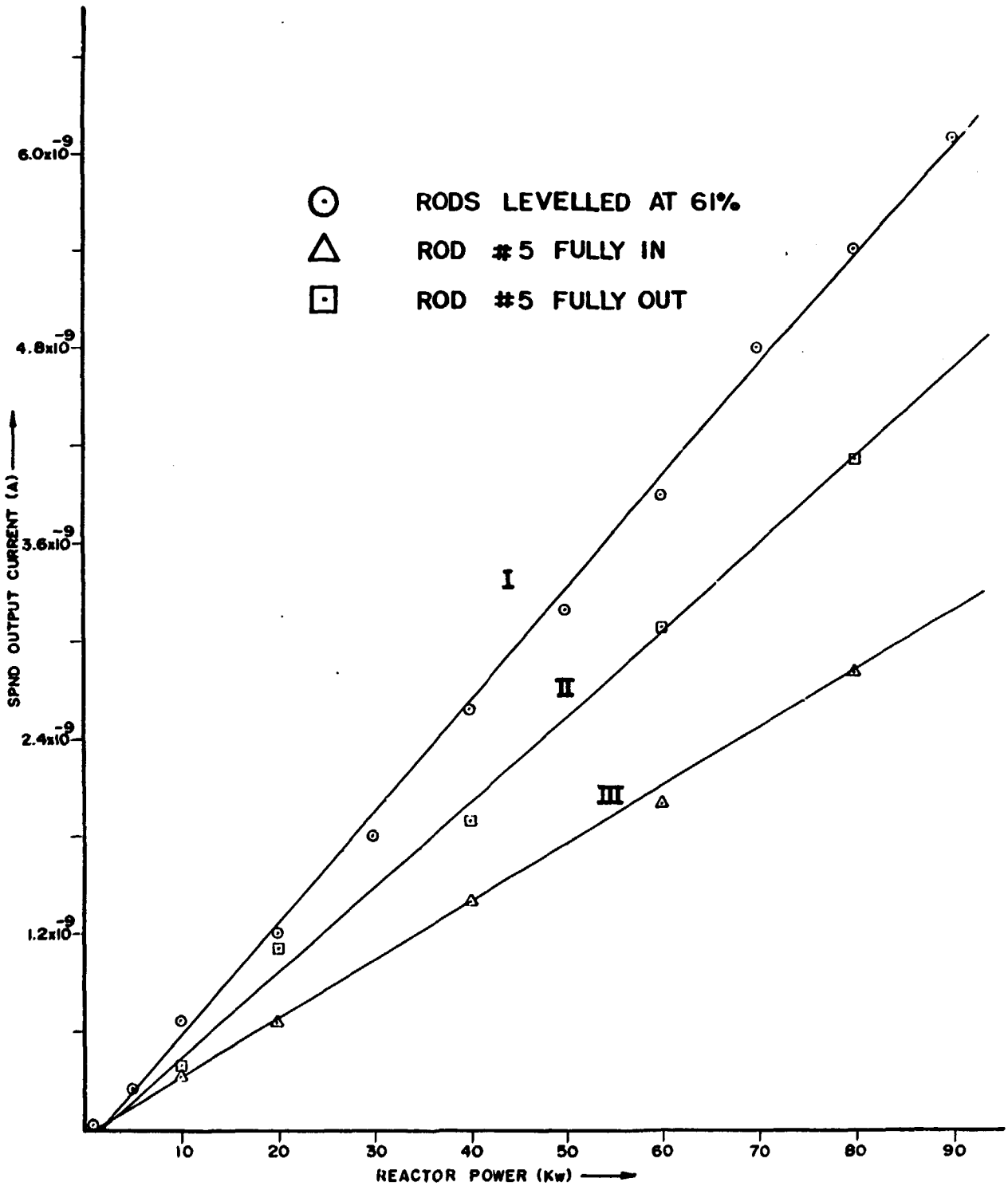

Fig. 5: Behaviour of SPND current with Reactor Power under Different Operating Conditions

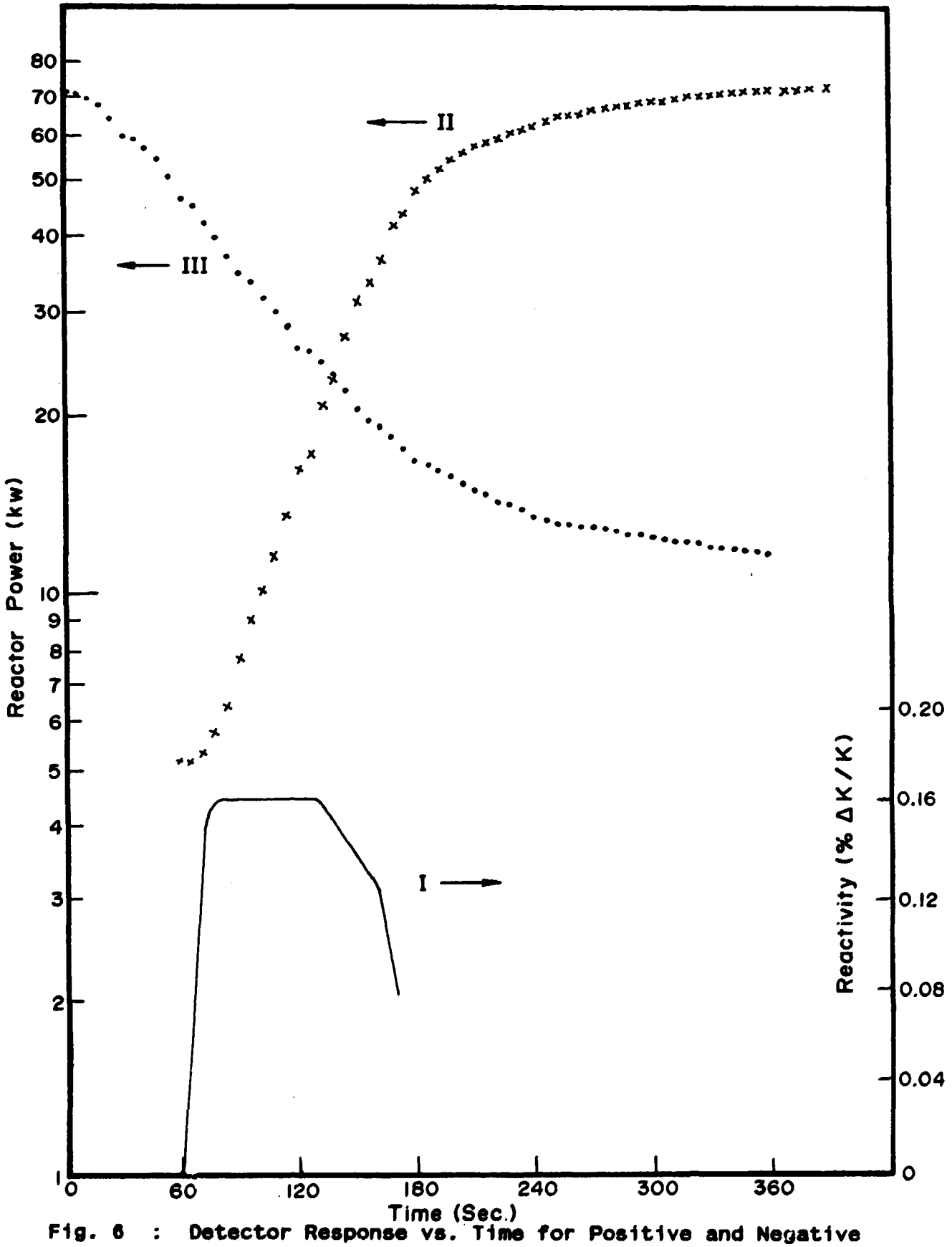

Fig. 6 : Detector Response vs. Time for Positive and Negative Reactivity inputs

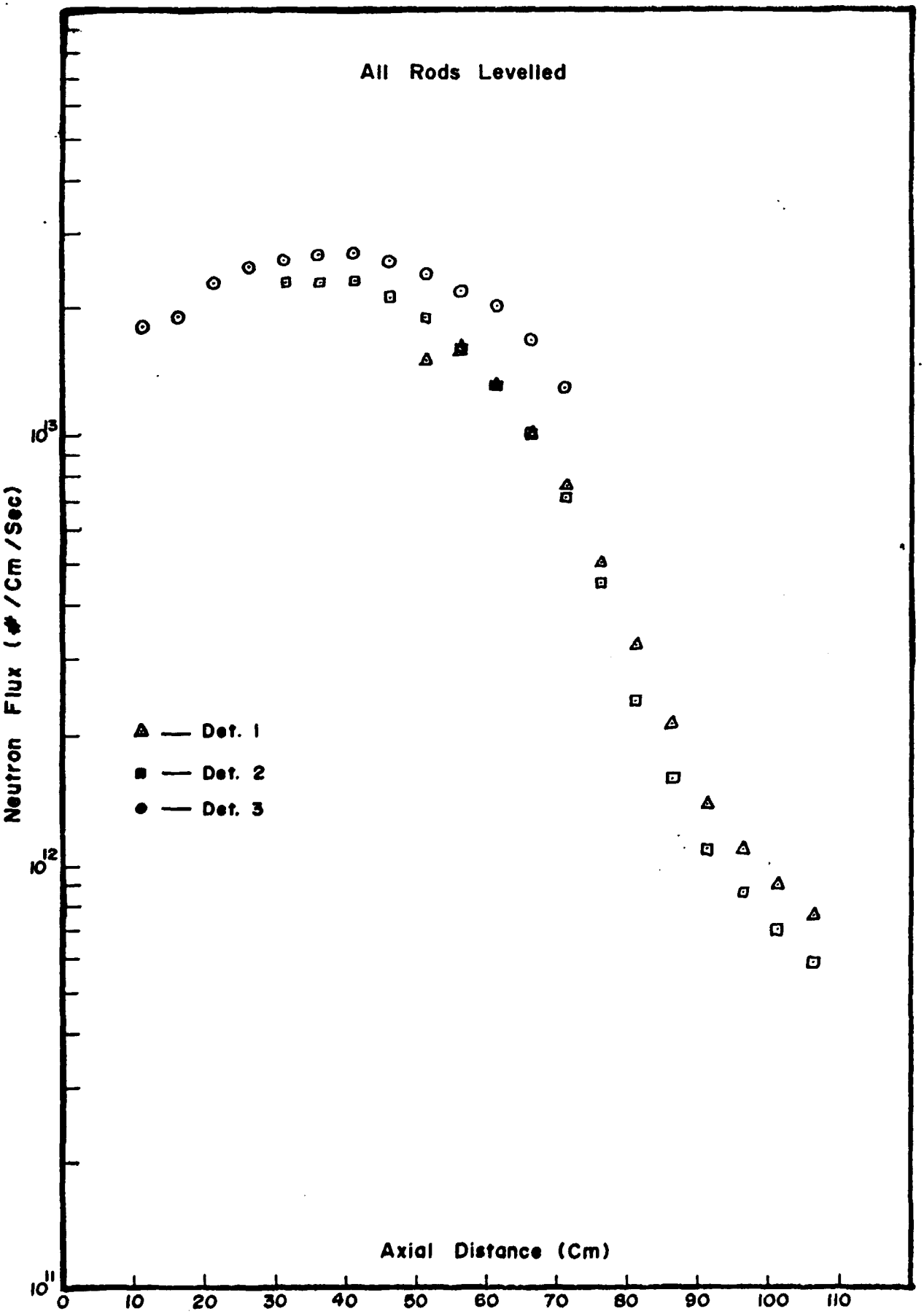

Fig. 7 : Axial Flux Distribution Obtained by the three Detectors with all Rods Levelled

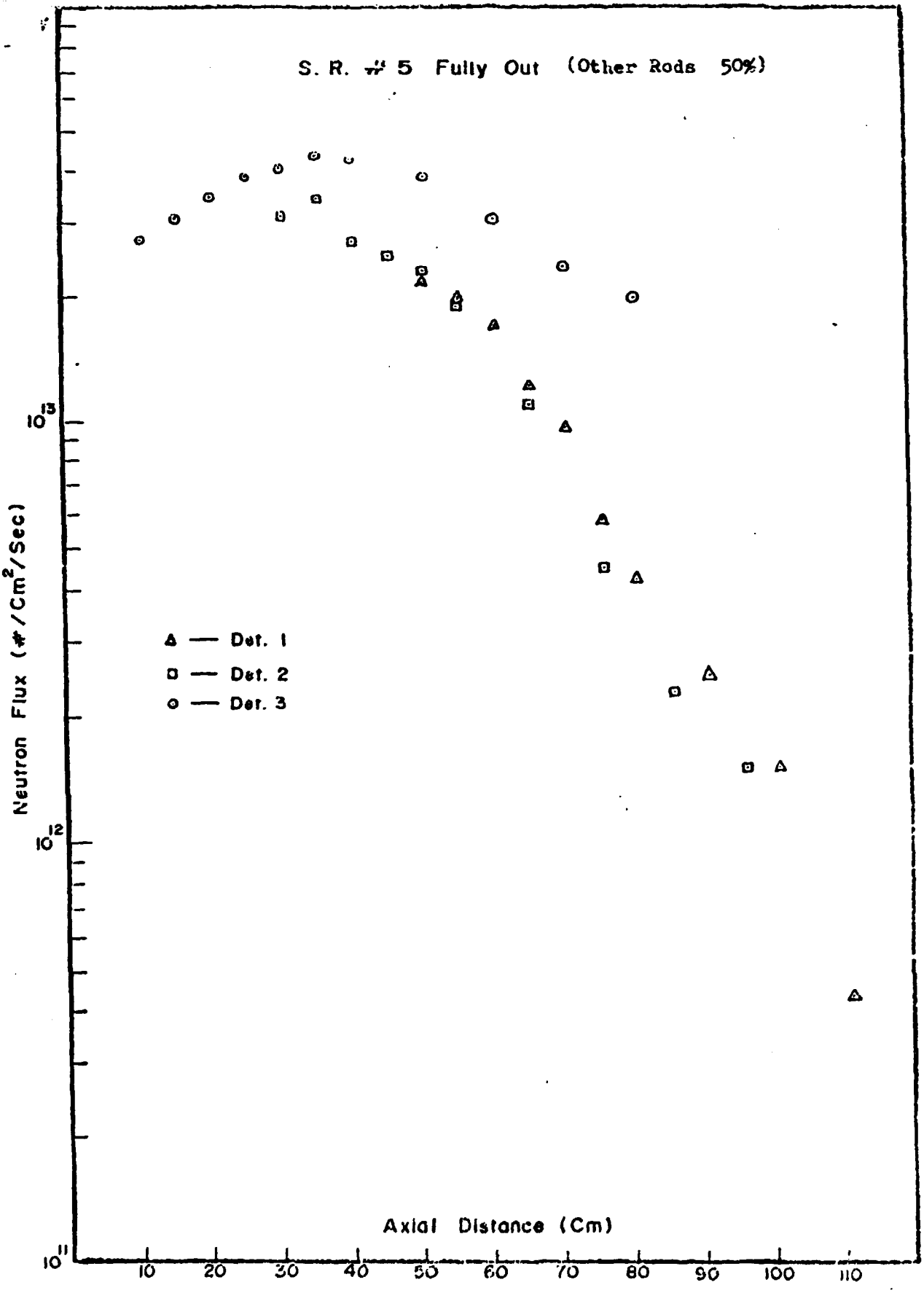

Fig. 8 : Axial Flux Distribution with Shim Rod no.5 Fully Out

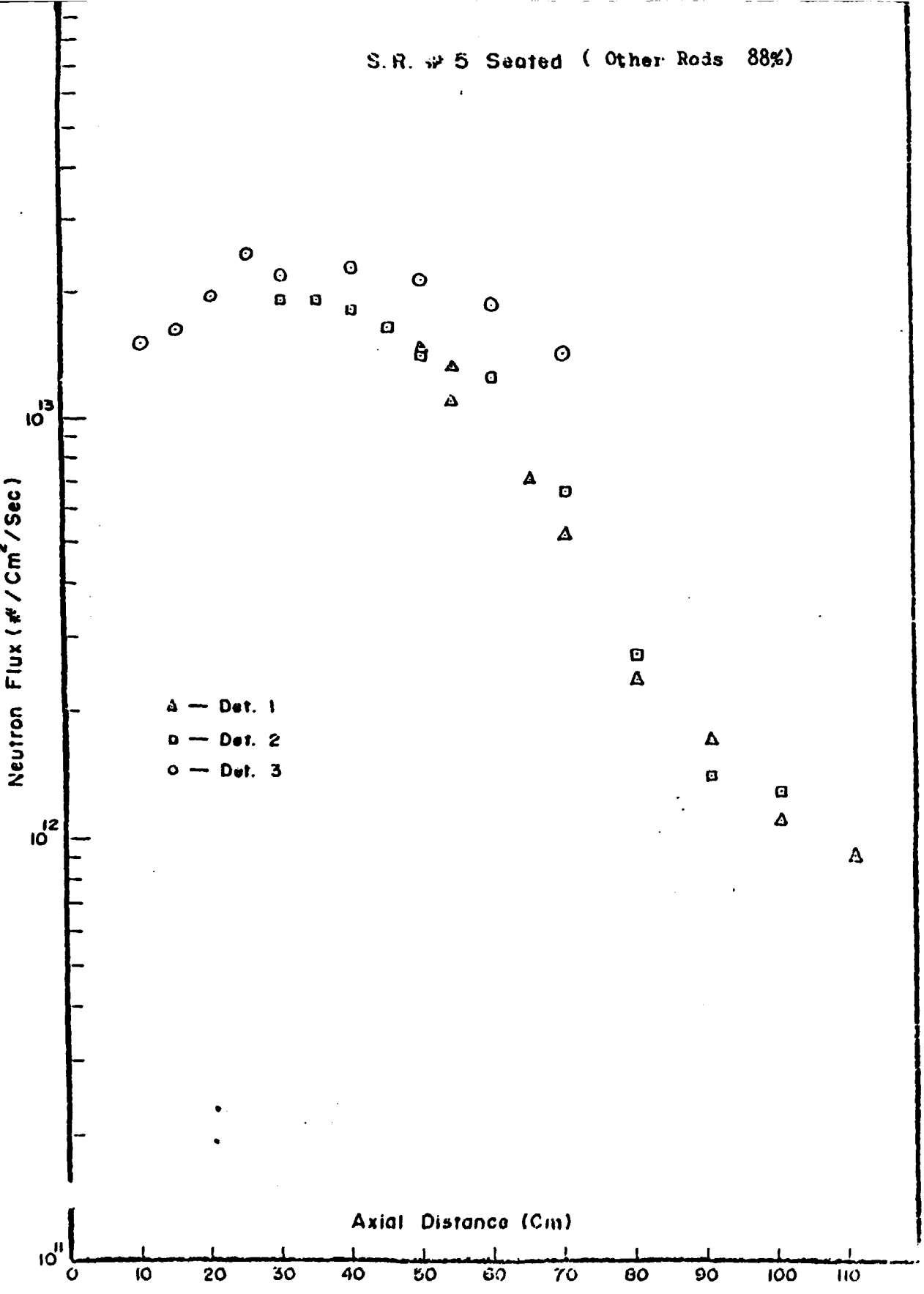

Fig. 9 : Axial Flux Distribution with Shim Rod no.5 Seated

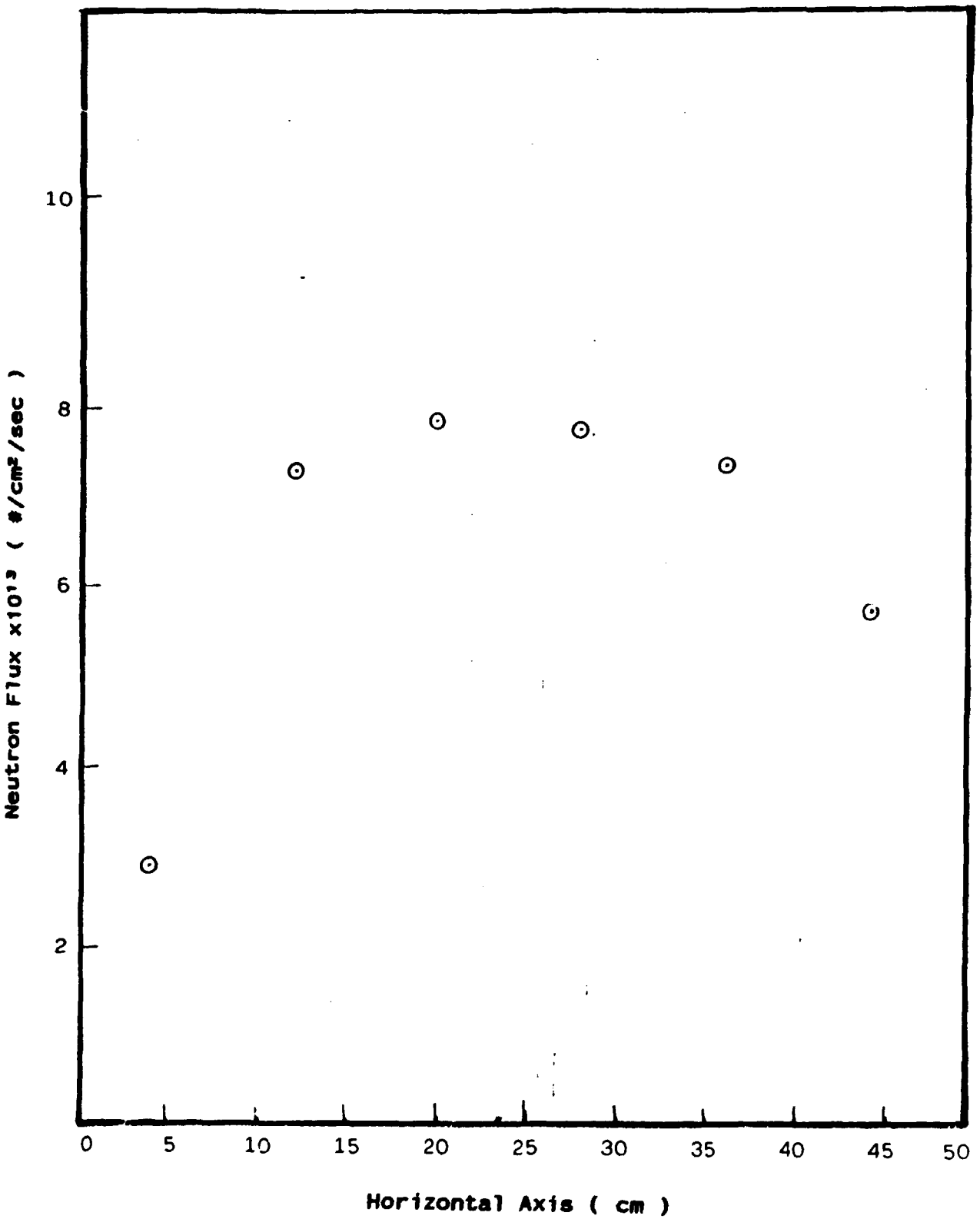

Fig. 10 : Horizontal Flux Distribution in the Water Reflector by the Middle Plane (no. 2) Detector

Acknowledgement

The authors wish to express their thanks to the reactor operators and supervisors for operating the reactor under different operating conditions as per requirements of the above measurements. Thanks are also due to Mr. Mannan of Activation Analysis Group of NCD for carrying out foil counting on their counting set-up.